Translational large animal model of hibernating myocardium: characterization by serial multimodal imaging

Juan Martínez-Milla, MD[1,2]; Carlos Galán-Arriola, DVM, PhD[1,3]; Manuel Carnero, MD, PhD[1,4]; Javier Cobiella, MD[1,4]; Daniel Pérez-Camargo, MD[1,4]; Victor Bautista-Hernández[1,5], MD PhD; Montse Rigol[3,6], PhD; Nuria Solanes[3,6], PhD; Rocío Villena-Gutierrez, MBs[1]; Manuel Lobo, MD[1]; Jesús Mateo, PhD[1]; Jean Paul Vilchez-Tschischke, MD PhD[1,7]; Beatriz Salinas, PhD[1,8,9]; Lorena Cussó, PhD[1,8,9]; Gonzalo Javier López, RT[1]; Valentín Fuster, MD PhD[1,10]; Manuel Desco, MD PhD[1,8,9]; Javier Sanchez-González, PhD[11]; Borja Ibanez, MD, PhD[1,2,3].

1. Centro Nacional de Investigaciones Cardiovasculares. Madrid Spain
2. Department of Cardiology. IIS- Hospital Universitario Fundación Jiménez Díaz. Madrid. Spain
3. Centro de Investigación Biomédica en Red en Enfermedades Cardiovasculares (CIBERCV), Madrid, Spain
4. Department of Cardiovascular Surgery. Hospital Clínico San Carlos. Madrid. Spain
5. Complejo Hospitalario Universitario A Coruña, Spain.
6. August Pi i Sunyer Biomedical Research Institute (IDIBAPS), Institut de Malalties Cardiovasculars, Hospital Clínic de Barcelona, Universitat de Barcelona, Spain
7. Department of Cardiology. Complejo Hospitalario Ruber Juan Bravo. Madrid. Spain
8. Departamento de Bioingeniería e Ingeniería Aeroespacial, Universidad Carlos III de Madrid, Madrid, Spain Instituto de Investigación Sanitaria Gregorio Marañón. Madrid, Spain
9. Centro de Investigación Biomédica en Red de Salud Mental (CIBERSAM), Spain
10. Zena and Michael A. Wiener Cardiovascular Institute, Icahn School of Medicine at Mount Sinai, New York, New York
11. Philips Healthcare, Madrid, Spain

Address for correspondence:

Borja Ibanez, MD PhD FESC. Translational Laboratory for Cardiovascular Imaging and Therapy, Centro Nacional de Investigaciones Cardiovasculares Carlos III (CNIC) & Cardiology Dpt, IIS-Fundación Jiménez Díaz. C/ Melchor Fernandez Almagro, 3, 28029 Madrid, Spain. Phone: +34 914531200.

Email: bibanez@cnic.es

Abstract:

Nonrevascularizable coronary artery disease is a frequent cause of hibernating myocardium leading to heart failure (HF). Currently there is paucity of therapeutic options for patients with this condition. There is a lack of animal models resembling clinical features of hibernating myocardium. Here we present a large animal model of hibernating myocardium characterized by serial multimodality imaging.

Yucatan minipigs underwent a surgical casein ameroid implant around proximal left anterior descending coronary artery (LAD), resulting in a progressive obstruction of the vessel. Pigs underwent serial multimodality imaging including invasive coronary angiography, cardiac magnetic resonance (CMR), and hybrid ^{18}F-Fluorodeoxyglucose positron emission tomography-computed tomography (FDG-PET/CT).

A total of 43 pigs were operated on and were followed for 120±37 days with monthly multimodality imaging. 24 pigs (56%) died during the follow-up. Severe LAD luminal stenosis was documented in all survivors. In the group of 19 long-term survivors, 17 (90%) developed left ventricular systolic dysfunction (median LVEF of 35% (IQR 32.5-40.5%)). In 17/17, at risk territory was viable on CMR and 14 showed an increased glucose uptake in the at-risk myocardium on ^{18}FDG-PET/CT.

The present pig model resembles most of the human hibernated myocardium characteristics and associated heart failure (systolic dysfunction, viable myocardium, and metabolic switch to glucose). This human-like model might be used to test novel interventions for nonrevascularizable coronary artery disease and ischemia heart failure as a previous stage to clinical trials.

Key Words: Hibernating myocardium; Heart Failure; Dilated Cardiomyopathy; Large animal models; Metabolic Switch; ^{18}FDG-PET/CT; Cardiac Magnetic Resonance.

Acknowledgements, Funding Sources

This study has been partially funded by the Horizon 2020 European Research Area Network on Cardiovascular Diseases (ERA-CVD) Joint Transnational Call “AC16/00021: FAT4HEART”, by the Spanish Society of Cardiology through a “Translational Research grant 2019”, and by the Instituto de Salud Carlos III (ISCIII) and the European Regional

Development Fund (ERDF) through a FIS grant (Ref # PI16/02110). Imaging phenotyping was partially supported by the Comunidad de Madrid (S2017/BMD-3867 RENIM-CM) and cofunded with European structural and investment funds. The CNIC is supported by the ISCIII, the Ministerio de Ciencia e Innovación and the Pro CNIC Foundation, and is a Severo Ochoa Center of Excellence (SEV-2015-0505).

Background

Ischemic heart disease (IHD) secondary to coronary artery disease (CAD) is a leading cause of morbidity and mortality worldwide and a frequent cause of heart failure (HF)[13, 23]. The prevalence of HF in developed countries is around 2% and it is estimated that about 150 million live with chronic HF worldwide[34].

Although percutaneous and surgical revascularizations have shown to be beneficial in CAD, these procedures are not always feasible, specially due to diffusely diseased vessels, leading to hibernating myocardium[15, 16]. Hibernating myocardium is a form of IHD in which left ventricular (LV) contraction is depressed, but ischemic myocardium remains viable[14]. Hibernating myocardium is the underlying cause of a significant proportion of HF with reduced ejection fraction (HFrEF)[25].

Cardiomyocytes metabolic reprogramming, characterized by a shift from fatty acids to glucose utilization as the preferential substrate, is a common phenomenon in different forms of HFrEF, including hibernated myocardium[6, 29]. In a mouse model of HF, metabolic switch has shown to be a potential therapeutic target[41]. The lack of large animal models of HF with accompanying metabolic switch confirming the rodent preliminary data limits the translational potential of this and future strategies.

Here we present the generation and deep phenotyping by serial multimodality imaging, of a pig model of hibernating myocardium with superimposed metabolic switch. This model can be useful for the HF community to test potential therapeutic targets as before entering the clinical arena.

Methods.

Study design

All animal studies were conducted at the CNIC and approved by the local CNIC Institutional Animal Research Committee, and the Regional Animal Research Committee. All animal procedures conformed to EU Directive 2010/63EU and Recommendation 2007/526/EC regarding the protection of animals used for experimental and other scientific purposes.

Study protocol in represented in Figure 1. Hibernating myocardium was induced in Yucatan Minipigs (35 -45 kg) by surgically placing a casein ameroid in the proximal left anterior descending (LAD) coronary artery. Casein ameroid generates a slowly progressive inwards stenosis as it is hydrated. First follow-up angiography was scheduled 30 days after surgery. Angiography was repeated every 2 weeks until severe stenosis (≥70%) and collateral circulation development was documented. At this time, pigs were scheduled for cardiac magnetic resonance (CMR). On CMR, hibernating myocardium was defined by the presence of reduced LVEF (<50%) in the absence of transmural late gadolinium enhancement (LGE <50% of transmurality). Pigs with evidence of hibernating myocardium were scheduled for ^{18}F-Fluorodeoxyglucose positron emission tomography/computed tomography (^{18}FDG-PET/CT) to evaluate the presence of metabolic switch in the LV anterior wall.

Surgical ameroid implant protocol

Animals were sedated by intramuscular injection of ketamine (20 mg/kg), xylazine (2 mg/kg) and midazolam (0.5 mg/kg). Then they were transferred to the operating room and placed on left lateral decubitus. Anesthesia was maintained with inhaled sevofluorane (3-4%) throughout all the procedure. Continuous intravenous fentanyl solution was infused as analgesia during the surgery. A left minitoracotomy was performed through the third or fourth intercostal space. Once in the pericardial cavity, the proximal LAD was located. To facilitate the exposure of this artery, a traction point was given on the left atrial appendage with a non-absorbable suture. Subsequently, a fine dissection of the LAD was performed and the ameroid ring implanted around the

proximal segment of the artery. Subsequently, the left atrial traction was removed, and hemostasis and flat closure performed (figure 2).

After the procedure, the animal was treated with dual anti-platelet therapy (aspirin plus clopidogrel) for one month to prevent LAD thrombosis. In order to try to reduce mortality in the perioperative period, which was presumably of arrhythmic origin; approximately halfway through the protocol (animal number 24) we decided to administer oral metoprolol twice daily for one month.

Invasive coronary angiography

Follow-up invasive coronary angiography was performed to evaluate the degree of LAD luminal stenosis induced by the progressive hydration of the ameroid, as well as the presence of collateral circulation. Pigs were sedated as described above, plus an intramuscular injection of buprenorphine (0.01 mg/kg) for analgesia. Through a percutaneous femoral artery access, left and right coronary arteries were engaged by diagnostic coronary catheters. Iodine contrast was injected, and several fluoroscopy projections recorded for each coronary artery.

CMR protocol

All studies were performed with a Philips 3-T Achieva Tx whole body scanner (Philips Healthcare, Best, The Netherlands) equipped with a 32-element phased-array cardiac coil. The CMR protocol included a standard segmented cine steady-state free-precession (SSFP) sequence to provide high-quality anatomical references, and T1 weighted LGE sequences.

The imaging parameters for the cine SSFP sequence were as follows: field of view (FOV) of 280 x 280 mm, slice thickness 6 mm with no gaps, repetition time (TR) 2.8 ms, echo time (TE) 1.4 ms, flip angle 45º, cardiac phases = 30, voxel size 1.8 x 1.8 mm, and number of excitations (NEX) = 3.

LGE imaging was performed 10-15 min after intravenous administration of 0.2 mM/kg gadopentetate dimeglumine contrast agent using an 3D inversion-recovery spoiled turbo field echo sequence (TR/TE/Flip angle= 2.4ms/1.13ms/10o) with an isotropic resolution of 1.5x1.5x1.5 mm3 on a FOV of 340x340x320 mm3 in the FH, LR, and AP directions. Data were acquired in mid-diastole with a 151.2 ms acquisition window.

Acquisition was accelerated using a net SENSE factor of 2.25 (1.5x1.5 in the AP and LR directions) with a bandwidth of 853Hz per-pixel. Inversion time was adjusted before acquisition using a look-locker scout sequence with different inversion times to ensure proper nulling of the healthy myocardium signal. For the analysis, 3D volume was reconstructed in short axis view with a slice thickness of 6mm. Cardiac quantitative perfusion was estimated using dynamic acquisition with dual-saturation recovery (TS=20, 80 ms) technique during gadolinium-based contrast administration (0.2 mmol) as previously described[33].

CMR analysis

CMR studies were analyzed by 2 experienced and independent observers using dedicated software (IntelliSpace Portal, Philips Healthcare, Best, the Netherlands). Briefly, LV cardiac borders were traced in each cine image to obtain LV end-diastolic mass, LV end-diastolic volume (LVEDV), end-systolic volume (LVESV), and LVEF. Wall thickening values for anterior and posterior contractility assessment were obtained as well from cardiac borders tracing. Late gadolinium-enhanced regions were defined as percentage of maximum myocardial signal intensity (full width at half maximum) and quantitatively analyzed. After perfusion map generation, regions of interest were analyzed in the anterior and posterior areas using dedicated software (MR Extended Work Space 2.6, Philips Healthcare).

^{18}FDG- PET/CT protocol

All studies were performed with GEMINI TF 64-slices PET-CT scan (Philips Healthcare, Best, the Netherlands). Animals were fasted 24 hours before the exams, having free access to water consumption, and glucose level was normalized to 100-150 mg/dL. Blood drops were drawn, and glucose was quantified using a CONTOURTM PLUS Blood Glucose Monitoring System. If glucose levels were <100 mg/dL, an intravenous (i.v.) bolus of saline with 50% glucose (5 mL bolus per 10 mg/dL below 100 mg/dL (e.g. 5 mL when glucose was 90-99mg/dL, 10 mL when glucose was 80-89, etc)). When glucose levels were >150 ml/dL, repeated blood draws were done every 15 min while the pig was resting until levels were in the target range. Glucose concentration had to remain in the target range for at least 30 min before radiotracer injection. PET studies were

acquired 40 minutes after i.v. administration of 370 MBq of ^{18}F-FDG. PET data were collected for 45-60 minutes with the animals anesthetized as described above and reconstructed. After the PET, a iodine contrast enhanced prospective ECG-gated cardiac CT was acquired using an X-ray kVp, and reconstructed to superpose the anatomical structures to ^{18}F-FDG distribution. PET-CT studies were analyzed using dedicated software (IntelliSpace Portal, Philips Healthcare, Best, The Netherlands) by placing a ROI in the anterior area and the posterior regions. Values were counts normalized to blood pool (ROI placed in descending thoracic aorta).

Histology

Animals were euthanized by intravenous injection of pentobarbital in overdose (50 mg/kg intravenously). After heart harvest, samples of the left ventricle (antero-septal and free lateral walls) were collected for histology. Samples were fixed in 4% formalin and then transferred to 70% ethanol. After paraffin embedding, 4 µm sections were cut and stained with hematoxylin & eosin.

Statistical analysis

Data are considered continuous variables and results are presented as median and interquartile range. LVEF was represented in a box plot in the follow-up. Box plots are used to represent LGE extension in percentage, wall thickening, quantitative perfusion and ^{18}F-FDG counts with median as central value and interquartile range as limits.

Results

Mortality associated with model induction

Of 43 pigs undergoing surgical ameroid implant, 24 (56%) died before the first scheduled coronary angiography (30 days after surgery). 15/43 pigs (35%) died within 24 hours of cardiac surgery. This mortality was attributed to surgical complications: 6 out of 15 died in the operating room due to refractory ventricular fibrillation or coronary rupture, the other 9 were found dead in cage. Two out of the 28 survivors (7%) were found dead in cage between day 1 and 7 after surgery. Finally, 7/26 pigs alive at day 7 were found dead in cage before the first scheduled coronary angiography (27%). No casualties were documented in pigs that were alive at day 30 Therefore, overall mortality of this model was 56% (Figure 3).

Hibernating myocardium phenotyping

Nineteen pigs arrived alive to the first angiography. Only 1 animal had severe LAD stenosis at the first angiography; in the others, severe LAD stenosis was found at the second or third angiography. Mean time to severe LAD stenosis diagnosis was 56±9 days (figure 4). Two pigs surviving to first scheduled angiography (day 30) did not show hibernating myocardium: one had normal LVEF, and another had low LVEF but transmural extension on LGE-CMR suggestive of absence of viability. 17 out of 19 pigs surviving to first scheduled angiography (89%) displayed all features of hibernating myocardium (severe stenosis of the LAD, LVEF<50% con CMR, absence of transmural delayed enhancement on LGE-CMR, and metabolic switch on PET/CT in 14/17 pigs) (Figure 5). On CMR, median LVEF of pigs with hibernating myocardium was 35% (IQR 32.5-40.5%) (Figure 6A). The extent of irreversible injury (LV mass with LGE) was 10% (IQR 8-13%) (Figure 6B). All pigs with hibernating myocardium had extensive regional wall motion abnormalities (akinesia / hypokinesia of one or more segments of the antero-septal wall (wall thickening 13% (IQR 1.2-21.3%)), with no alterations or mild hypokinesia in the posterior wall (wall thickening 47.5% (IQR 33-69.8%)) (Figure 6C&D). and viability on LGE-CMR (Figure 6B). In terms of quantitative perfusion, it was analyzed in the 17 alive pigs and the mean quantitative perfusion in anterior wall (hibernated myocardium) was 127.5 (IQR 116.5-140.5) ml/100g/min and in the posterior wall (remote myocardium) was 193 (IQR 166-211.5) ml/100g/min (Figure 6E&F). To better

define the viability of the ischemic myocardium (thus proving its hibernating nature), stress CMR with dobutamine infusion was performed in 3 animals[35, 36]. Global LVEF increased from 35% (IQR 33-37%) at baseline to 64% (IQR: 60-67%) under dobutamine infusion. Regional contractile evaluation showed an increased in contractile function both in the hibernating and remote areas: hibernating anteroseptal wall thickening increased from 13.5% (IQR: 7.7-19.3%) at baseline to 43.5% (IQR: 27.5-67%) under dobutamine infusion. Remote posterior wall thickening increased from 50% (IQR: 33.8-67.8%) at baseline to 93.8% (IQR: 84.8-103.8%) under dobutamine infusion. Figure 7 illustrates global and regional systolic improvement in all 3 animals during dobutamine infusion.

Metabolic Switch

From the 17 pigs displaying low LVEF and viability on LGE-CMR, 3 could not undergo ^{18}FDG-PET/CT due to technical issues. Three healthy pigs underwent the same ^{18}FDG-PET/CT protocol and served as controls. Thus, ^{18}FDG-PET/CT study to evaluate myocardial glucose uptake was performed in 14 pigs All 14 intervened pigs (100%) displayed an overt increase in glucose uptake in the ischemic, akinetic/hypokinetic LV area, as compared to the remote LV wall (Figure 6G&H). Glucose uptake in the 3 controls was homogeneous across the different LV regions, and lower than that of the hibernating myocardium of intervened pigs (Figure 6G&H).

Histology

One day after the PET/CT study, pigs were euthanized, and the heart harvested. Patchy replacement fibrosis was observed in the anterior and lateral LV wall (hibernating regions) but not in the remote myocardium (posterior wall). These areas of fibrosis were mainly found in coronal slice levels 3 and 4, and were accompanied by neovascularization (Figure 8).

Discussion

Here we have presented the phenotyping of a large animal model resembling most of the features of hibernating myocardium. By using serial, state-of-the-art, multimodality imaging, we show that pigs surviving 45 days after surgical implant of an ameroid around the LAD present severe coronary artery stenosis with low LVEF and a metabolic switch in the ischemic region.

Large animal models of chronic ischemia with hibernating myocardium are complex to develop due to the challenging interventions requiring multiple specific skills, and the long time needed to reach a full-blown phenotype. These models have been carried out mostly in mice, dogs and pigs.[2, 3, 10, 26, 27] According to the International Guidelines of Animal Models of Myocardial Ischemia, large animals and specifically the pig is the ideal one to test different evaluation techniques for myocardial perfusion, molecular biology underlying myocardial ischemia and cardiac metabolism[5, 17, 20, 24]. The pig offers numerous advantages, including a body mass-indexed heart weight very similar to that of the human, and a rapid development of the cardiovascular system (at 3-5 months of age, the pigs have fully developed autonomic nervous and vascular systems[7]). Opposed to other large animal models, pigs have a poorly developed network of coronary collateral circulation, favouring the development of hibernating myocardium upon progressive coronary stenosis[20, 30, 39].

There are two different approaches for the generation of chronic ischemia by inducing coronary artery stenosis: fixed severe stenosis during index surgery[19, 28], and progressive stenosis from surgery onwards[21]. Both techniques generate a flow limitation distal to the coronary artery segment intervened. Of both, the most widely extended technique for the development of hibernating myocardium is the progressive stenosis since it resembles better the development of hibernation in the clinical setting, which usually occurs as a progressive phenomenon. In previous models the most frequently intervened coronary artery is the left circumflex, since it is more accessible and the duration of intervention is shorter [21, 32]. We decided to intervene the LAD as the amount of myocardium supplied by this artery is larger and the chances to induce reduction in global LVEF are higher, as we demonstrated.

The model we presented has some pros and cons compared to others in the literature (mainly targeting the left circumflex artery). The pros include a final phenotype more

similar to the human scenario including a large ischemic area, affecting the anterior wall. Cons include a high mortality within the first weeks after intervention: close to 60% of pigs undergoing surgery die before showing a hibernating myocardium. This mortality rate is significantly higher to that reported for left circumflex models (25%)[22, 37, 38, 40]. One reason for the high mortality rate could be the acute thrombotic occlusion of the narrowed LAD. In order to reduce this possibility, we kept pigs under dual antiplatelet therapy for several weeks after surgery. Another potential reason was the larger amount of ischemic myocardium generated in the LAD approach, probably increasing the incidence of malignant arrhythmias; but when we decided to administer metoprolol, there was not any impact in the mortality. Other groups have performed an ameroid implant in the LAD with lower mortality rates[11, 22, 38], but the level of the ameroid implant was more distal than in ours, thus generating a smaller ischemic region. Myocardial phenotyping of models of hibernated myocardium has been mainly done by echocardiography, thus allowing only a cardiac motion evaluation[9, 19, 22]. To date no study has performed a comprehensive tissue characterization study like the one presented here. The use of CMR and PET/CT allows a very comprehensive characterization of the ischemic myocardium beyond cardiac contractility. The confirmation of myocardial viability and the demonstration of a metabolic switch clearly shows the high translational potential of this model. In physiological conditions, the myocardium uses fatty acids as the main metabolic substrate. A metabolic switch characterized by a change from fatty acids to glucose as the preferred substrate is a condition observed in heart failure from different etiologies, including hibernating myocardium. We used ^{18}F-FDG radiotracer to be able to compare the ischemic and the remote regions in terms of glucose uptake. ^{18}F-FDG is a widespread used radiotracer due to its long half-life (approximately 2 hours) and the good quality of the PET images obtained[31]. Despite we did not measure fatty acids uptake directly, the clear differences in glucose uptake from different myocardial regions is high suggestive of a metabolic switch. There are different tracers used to evaluate beta-oxidation of fatty acids by the myocardium, such as 14- (R, S) -18F-fluoro-6 thiaheptadecanoic acid (FTHA) or 18F-fluoro-4-thia-palmitate (FTP); however, these tracers are difficult to be used in large animal experiments due to the important economic costs[31].

Our long-term ambition is to use this model to test different therapies suited for heart failure in general and for hibernating myocardium in particular. Interventions able to revert the metabolic switch have been proposed in small animal studies[41]. We plan to perform a preclinical trial in pigs with a metabolic intervention. Furthermore, this model is ideal to test strategies able to induce enhanced neovascularization, such as cell therapy[1, 4], gene therapy or pharmacological therapies.

Study Limitations

The present study has some limitations. The main limitation of this model is the high mortality associated with it before hibernating myocardium is documented. As commented, we have not measured directly fatty acids uptake by the myocardium, and thus the demonstration of metabolic switch is indirect. The evaluation of myocardial viability was performed by the accepted LGE-CMR approach; however, the presence of contractile reserve was only confirmed in 3 pigs. Pigs were not revascularized to demonstrate the full reversibility of cardiac dysfunction, as it is expected for hibernating myocardium. The surgical revascularization of pigs with an ameroid implanted months before is a very challenging intervention. While previous studies have reported different models of hibernating myocardium[2, 3, 10, 26, 27], thus partially limiting the novelty of our work, ours is the first one to provide a comprehensive longitudinal multimodality evaluation. Our histology analysis is limited and we have not performed electron microscopy to evaluate typical features associated with hibernated myocardium such as glycogen droplets, doughnut mitochondria, and loss of myofibrils quantification[8, 18]. Our model is aimed at serving as a tool to test novel therapeutic interventions in the future, but as presented lacks of novel mechanistic insights into the hibernating myocardium condition. Translation of pig studies to humans is complex not only because of the lack of comorbidities in the former, but also because the underlying signal transduction of disease state and that of therapeutic strategies is not necessarily equal[12].

References

1. Alvino VV, Fernandez-Jimenez R, Rodriguez-Arabaolaza I, Slater S, Mangialardi G, Avolio E, Spencer H, Culliford L, Hassan S, Sueiro Ballesteros L, Herman A, Ayaon-Albarran A, Galan-Arriola C, Sanchez-Gonzalez J, Hennessey H, Delmege C, Ascione R, Emanueli C, Angelini GD, Ibanez B, Madeddu P (2018) Transplantation of Allogeneic Pericytes Improves Myocardial Vascularization and Reduces Interstitial Fibrosis in a Swine Model of Reperfused Acute Myocardial Infarction. Journal of the American Heart Association 7 doi:10.1161/JAHA.117.006727
2. Bito V, Heinzel FR, Weidemann F, Dommke C, van der Velden J, Verbeken E, Claus P, Bijnens B, De Scheerder I, Stienen GJ, Sutherland GR, Sipido KR (2004) Cellular mechanisms of contractile dysfunction in hibernating myocardium. Circ Res 94:794-801 doi:10.1161/01.RES.0000124934.84048.DF
3. Bito V, van der Velden J, Claus P, Dommke C, Van Lommel A, Mortelmans L, Verbeken E, Bijnens B, Stienen G, Sipido KR (2007) Reduced force generating capacity in myocytes from chronically ischemic, hibernating myocardium. Circ Res 100:229-237 doi:10.1161/01.RES.0000257829.07721.57
4. Bobi J, Solanes N, Fernandez-Jimenez R, Galan-Arriola C, Dantas AP, Fernandez-Friera L, Galvez-Monton C, Rigol-Monzo E, Aguero J, Ramirez J, Roque M, Bayes-Genis A, Sanchez-Gonzalez J, Garcia-Alvarez A, Sabate M, Roura S, Ibanez B, Rigol M (2017) Intracoronary Administration of Allogeneic Adipose Tissue-Derived Mesenchymal Stem Cells Improves Myocardial Perfusion But Not Left Ventricle Function, in a Translational Model of Acute Myocardial Infarction. Journal of the American Heart Association 6 doi:10.1161/JAHA.117.005771
5. Botker HE, Hausenloy D, Andreadou I, Antonucci S, Boengler K, Davidson SM, Deshwal S, Devaux Y, Di Lisa F, Di Sante M, Efentakis P, Femmino S, Garcia-Dorado D, Giricz Z, Ibanez B, Iliodromitis E, Kaludercic N, Kleinbongard P, Neuhauser M, Ovize M, Pagliaro P, Rahbek-Schmidt M, Ruiz-Meana M, Schluter KD, Schulz R, Skyschally A, Wilder C, Yellon DM, Ferdinandy P, Heusch G (2018) Practical guidelines for rigor and reproducibility in preclinical and clinical studies on cardioprotection. Basic Res Cardiol 113:39 doi:10.1007/s00395-018-0696-8
6. Braunwald E (2013) Research advances in heart failure: a compendium. Circ Res 113:633-645 doi:10.1161/CIRCRESAHA.113.302254
7. Buckley NM, Gootman PM, Yellin EL, Brazeau P (1979) Age-related cardiovascular effects of catecholamines in anesthetized piglets. Circ Res 45:282-292 doi:10.1161/01.res.45.2.282
8. Cabrera JA, Butterick TA, Long EK, Ziemba EA, Anderson LB, Duffy CM, Sluiter W, Duncker DJ, Zhang J, Chen Y, Ward HB, Kelly RF, McFalls EO (2013) Reduced expression of mitochondrial electron transport chain proteins from hibernating hearts relative to ischemic preconditioned hearts in the second window of protection. J Mol Cell Cardiol 60:90-96 doi:10.1016/j.yjmcc.2013.03.018
9. Caillaud D, Calderon J, Reant P, Lafitte S, Dos Santos P, Couffinhal T, Roques X, Barandon L (2010) Echocardiographic analysis with a two-dimensional strain of chronic myocardial ischemia induced with ameroid constrictor in the pig. Interact Cardiovasc Thorac Surg 10:689-693 doi:10.1510/icvts.2010.232819

10. Canty JM, Jr., Klocke FJ (1987) Reductions in regional myocardial function at rest in conscious dogs with chronically reduced regional coronary artery pressure. Circ Res 61:II107-116
11. Fallavollita JA, Logue M, Canty JM, Jr. (2001) Stability of hibernating myocardium in pigs with a chronic left anterior descending coronary artery stenosis: absence of progressive fibrosis in the setting of stable reductions in flow, function and coronary flow reserve. J Am Coll Cardiol 37:1989-1995 doi:10.1016/s0735-1097(01)01250-5
12. Gedik N, Kruger M, Thielmann M, Kottenberg E, Skyschally A, Frey UH, Cario E, Peters J, Jakob H, Heusch G, Kleinbongard P (2017) Proteomics/phosphoproteomics of left ventricular biopsies from patients with surgical coronary revascularization and pigs with coronary occlusion/reperfusion: remote ischemic preconditioning. Sci Rep 7:7629 doi:10.1038/s41598-017-07883-5
13. Gheorghiade M, Sopko G, De Luca L, Velazquez EJ, Parker JD, Binkley PF, Sadowski Z, Golba KS, Prior DL, Rouleau JL, Bonow RO (2006) Navigating the crossroads of coronary artery disease and heart failure. Circulation 114:1202-1213 doi:10.1161/CIRCULATIONAHA.106.623199
14. Heusch G, Libby P, Gersh B, Yellon D, Bohm M, Lopaschuk G, Opie L (2014) Cardiovascular remodelling in coronary artery disease and heart failure. Lancet 383:1933-1943 doi:10.1016/S0140-6736(14)60107-0
15. Heusch G, Schulz R (1996) Hibernating myocardium: a review. J Mol Cell Cardiol 28:2359-2372 doi:10.1006/jmcc.1996.0229
16. Heusch G, Schulz R, Rahimtoola SH (2005) Myocardial hibernation: a delicate balance. Am J Physiol Heart Circ Physiol 288:H984-999 doi:10.1152/ajpheart.01109.2004
17. Heusch G, Skyschally A, Schulz R (2011) The in-situ pig heart with regional ischemia/reperfusion - ready for translation. J Mol Cell Cardiol 50:951-963 doi:10.1016/j.yjmcc.2011.02.016
18. Holley CT, Long EK, Butterick TA, Duffy CM, Lindsey ME, Stone LH, McFalls EO, Kelly RF (2015) Mitochondrial fusion proteins in revascularized hibernating hearts. J Surg Res 195:29-36 doi:10.1016/j.jss.2014.12.052
19. Hughes GC, Post MJ, Simons M, Annex BH (2003) Translational physiology: porcine models of human coronary artery disease: implications for preclinical trials of therapeutic angiogenesis. J Appl Physiol (1985) 94:1689-1701 doi:10.1152/japplphysiol.00465.2002
20. Ibanez B, Aletras AH, Arai AE, Arheden H, Bax J, Berry C, Bucciarelli-Ducci C, Croisille P, Dall'Armellina E, Dharmakumar R, Eitel I, Fernandez-Jimenez R, Friedrich MG, Garcia-Dorado D, Hausenloy DJ, Kim RJ, Kozerke S, Kramer CM, Salerno M, Sanchez-Gonzalez J, Sanz J, Fuster V (2019) Cardiac MRI Endpoints in Myocardial Infarction Experimental and Clinical Trials: JACC Scientific Expert Panel. J Am Coll Cardiol 74:238-256 doi:10.1016/j.jacc.2019.05.024
21. Inou T, Tomoike H, Watanabe K, Kikuchi Y, Mizukami M, Kurozumi T, Nakamura M (1980) A newly developed X-ray transparent ameroid constrictor for study on progression of gradual coronary stenosis. Basic Res Cardiol 75:537-543 doi:10.1007/bf01907835
22. Keeran KJ, Jeffries KR, Zetts AD, Taylor J, Kozlov S, Hunt TJ (2017) A Chronic Cardiac Ischemia Model in Swine Using an Ameroid Constrictor. J Vis Exp doi:10.3791/56190

23. Khatibzadeh S, Farzadfar F, Oliver J, Ezzati M, Moran A (2013) Worldwide risk factors for heart failure: a systematic review and pooled analysis. Int J Cardiol 168:1186-1194 doi:10.1016/j.ijcard.2012.11.065
24. Lindsey ML, Bolli R, Canty JM, Jr., Du XJ, Frangogiannis NG, Frantz S, Gourdie RG, Holmes JW, Jones SP, Kloner RA, Lefer DJ, Liao R, Murphy E, Ping P, Przyklenk K, Recchia FA, Schwartz Longacre L, Ripplinger CM, Van Eyk JE, Heusch G (2018) Guidelines for experimental models of myocardial ischemia and infarction. Am J Physiol Heart Circ Physiol 314:H812-H838 doi:10.1152/ajpheart.00335.2017
25. Lozano I, Capin E, de la Hera JM, Llosa JC, Carro A, Lopez-Palop R (2015) Diffuse Coronary Artery Disease Not Amenable to Revascularization: Long-term Prognosis. Rev Esp Cardiol (Engl Ed) 68:631-633 doi:10.1016/j.rec.2015.02.013
26. McFalls EO, Kelly RF, Hu Q, Mansoor A, Lee J, Kuskowski M, Sikora J, Ward HB, Zhang J (2007) The energetic state within hibernating myocardium is normal during dobutamine despite inhibition of ATP-dependent potassium channel opening with glibenclamide. Am J Physiol Heart Circ Physiol 293:H2945-2951 doi:10.1152/ajpheart.00012.2007
27. McFalls EO, Murad B, Haspel HC, Marx D, Sikora J, Ward HB (2003) Myocardial glucose uptake after dobutamine stress in chronic hibernating swine myocardium. J Nucl Cardiol 10:385-394 doi:10.1016/s1071-3581(03)00431-8
28. Millard RW (1981) Induction of functional coronary collaterals in the swine heart. Basic Res Cardiol 76:468-473 doi:10.1007/bf01908345
29. Neubauer S (2007) The failing heart--an engine out of fuel. N Engl J Med 356:1140-1151 doi:10.1056/NEJMra063052
30. Patterson RE, Kirk ES (1983) Analysis of coronary collateral structure, function, and ischemic border zones in pigs. Am J Physiol 244:H23-31 doi:10.1152/ajpheart.1983.244.1.H23
31. Peterson LR, Gropler RJ (2010) Radionuclide imaging of myocardial metabolism. Circ Cardiovasc Imaging 3:211-222 doi:10.1161/CIRCIMAGING.109.860593
32. Roth DM, Maruoka Y, Rogers J, White FC, Longhurst JC, Bloor CM (1987) Development of coronary collateral circulation in left circumflex Ameroid-occluded swine myocardium. Am J Physiol 253:H1279-1288 doi:10.1152/ajpheart.1987.253.5.H1279
33. Sanchez-Gonzalez J, Fernandez-Jimenez R, Nothnagel ND, Lopez-Martin G, Fuster V, Ibanez B (2015) Optimization of dual-saturation single bolus acquisition for quantitative cardiac perfusion and myocardial blood flow maps. J Cardiovasc Magn Reson 17:21 doi:10.1186/s12968-015-0116-2
34. Sayago-Silva I, Garcia-Lopez F, Segovia-Cubero J (2013) Epidemiology of heart failure in Spain over the last 20 years. Rev Esp Cardiol (Engl Ed) 66:649-656 doi:10.1016/j.rec.2013.03.012
35. Schulz R, Guth BD, Pieper K, Martin C, Heusch G (1992) Recruitment of an inotropic reserve in moderately ischemic myocardium at the expense of metabolic recovery. A model of short-term hibernation. Circ Res 70:1282-1295 doi:10.1161/01.res.70.6.1282
36. Schulz R, Miyazaki S, Miller M, Thaulow E, Heusch G, Ross J, Jr., Guth BD (1989) Consequences of regional inotropic stimulation of ischemic myocardium on regional myocardial blood flow and function in anesthetized swine. Circ Res 64:1116-1126 doi:10.1161/01.res.64.6.1116
37. St Louis JD, Hughes GC, Kypson AP, DeGrado TR, Donovan CL, Coleman RE, Yin B, Steenbergen C, Landolfo KP, Lowe JE (2000) An experimental model of

chronic myocardial hibernation. Ann Thorac Surg 69:1351-1357 doi:10.1016/s0003-4975(00)01130-9
38. Tarkia M, Stark C, Haavisto M, Kentala R, Vahasilta T, Savunen T, Strandberg M, Hynninen VV, Saunavaara V, Tolvanen T, Teras M, Rokka J, Pietila M, Saukko P, Roivainen A, Saraste A, Knuuti J (2015) Cardiac remodeling in a new pig model of chronic heart failure: Assessment of left ventricular functional, metabolic, and structural changes using PET, CT, and echocardiography. J Nucl Cardiol 22:655-665 doi:10.1007/s12350-015-0068-9
39. Tsang HG, Rashdan NA, Whitelaw CB, Corcoran BM, Summers KM, MacRae VE (2016) Large animal models of cardiovascular disease. Cell Biochem. Funct. 34:113-132 doi:10.1002/cbf.3173
40. Unger EF (2001) Experimental evaluation of coronary collateral development. Cardiovasc Res 49:497-506 doi:10.1016/s0008-6363(00)00285-6
41. Wai T, Garcia-Prieto J, Baker MJ, Merkwirth C, Benit P, Rustin P, Ruperez FJ, Barbas C, Ibanez B, Langer T (2015) Imbalanced OPA1 processing and mitochondrial fragmentation cause heart failure in mice. Science 350:aad0116 doi:10.1126/science.aad0116

Figure Legends

<u>Figure 1</u>. Study protocol.

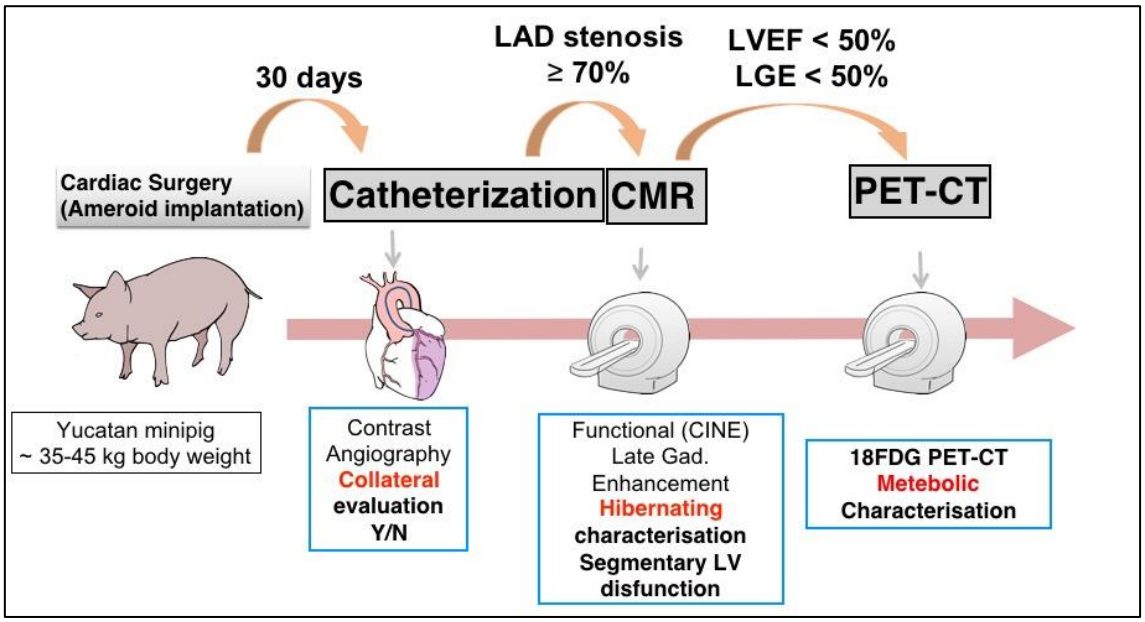

Figure 2. Surgical technique.

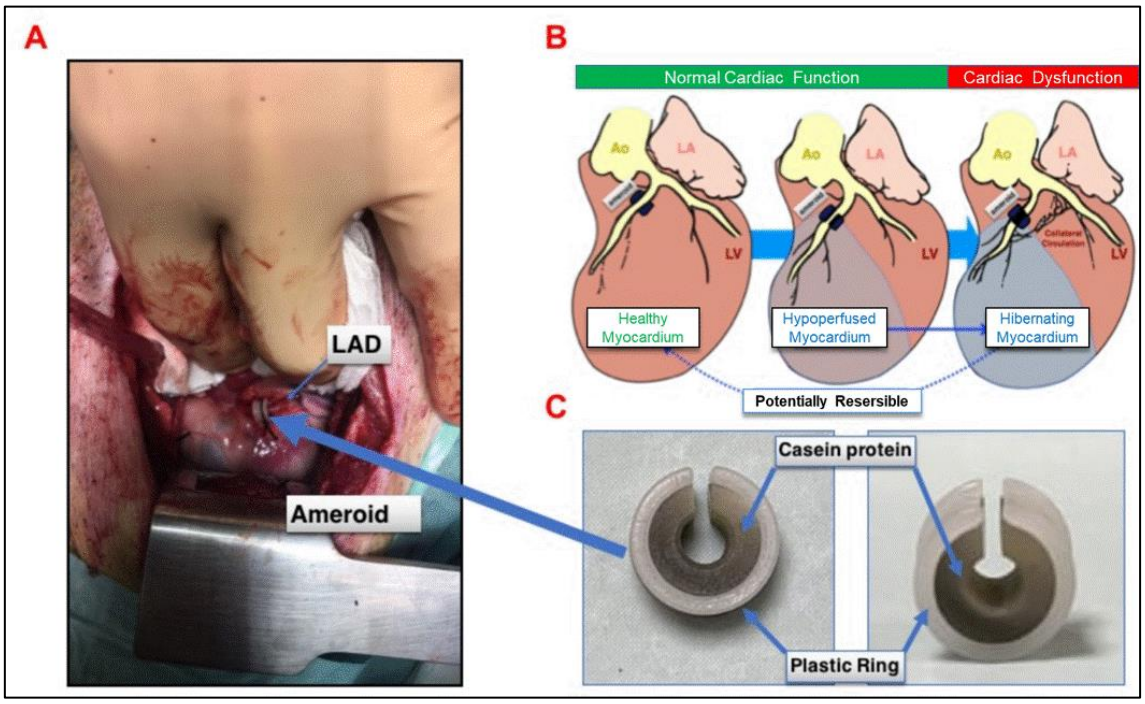

A: Surgical field for ameroid implant around the LAD. B: Representation of the left ventricular systolic disfunction across time after ameroid implantation. C: Image of the ameroid showing its components

Figure 3. **Time line of mortality associated with the model.**

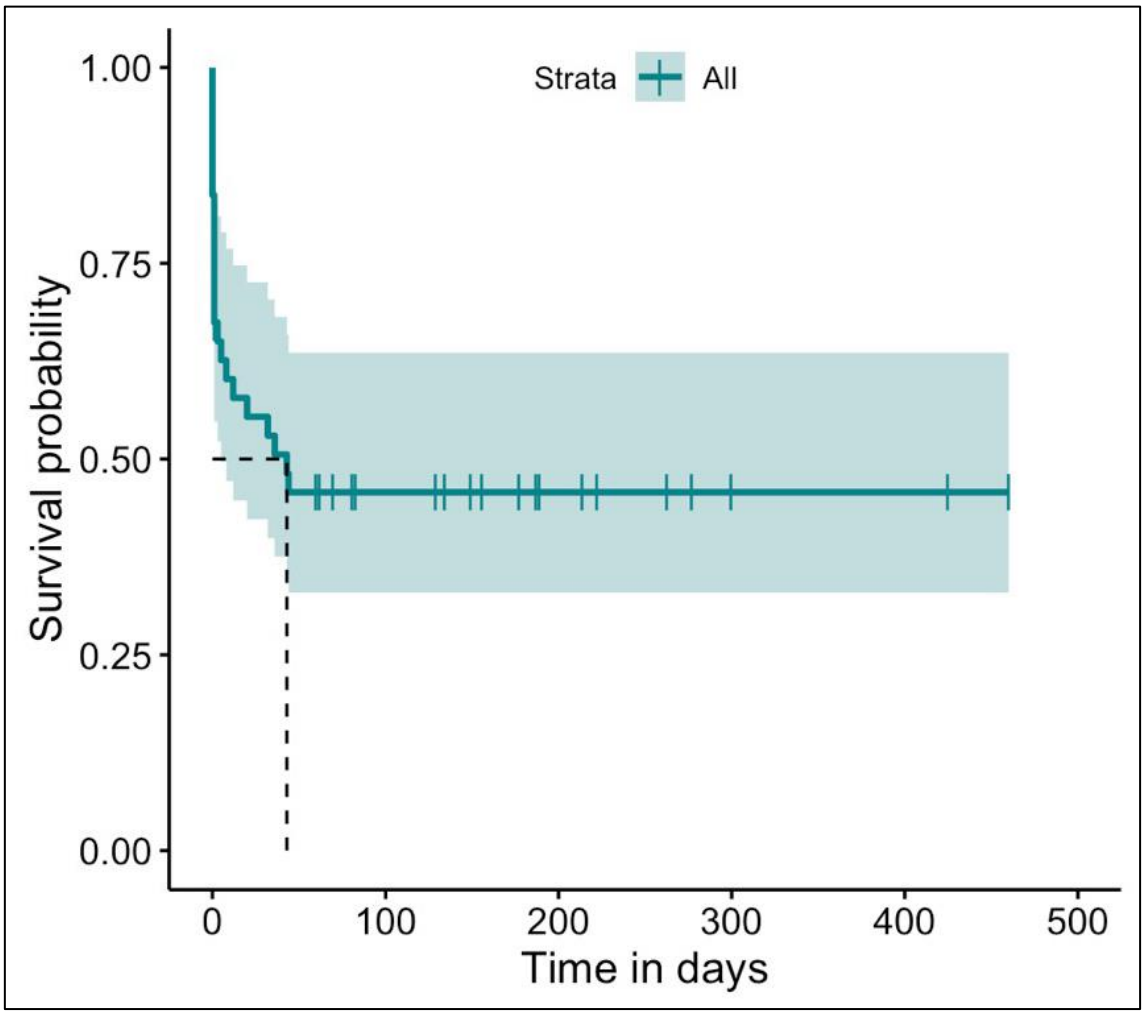

Figure 4. Kaplan-Meier curve showing time to severe LAD stenosis.

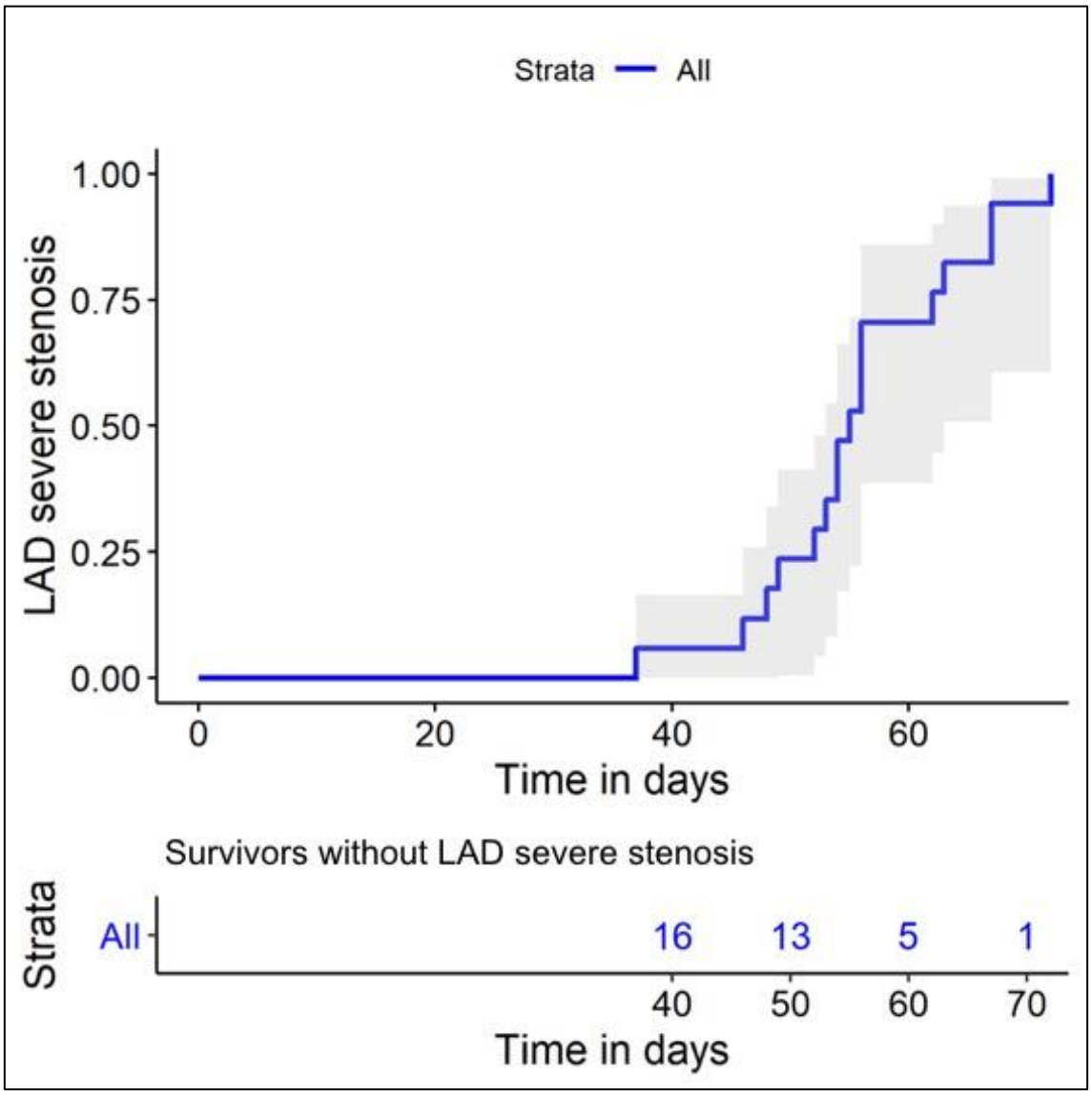

Figure 5. Representative case of hibernating myocardium.

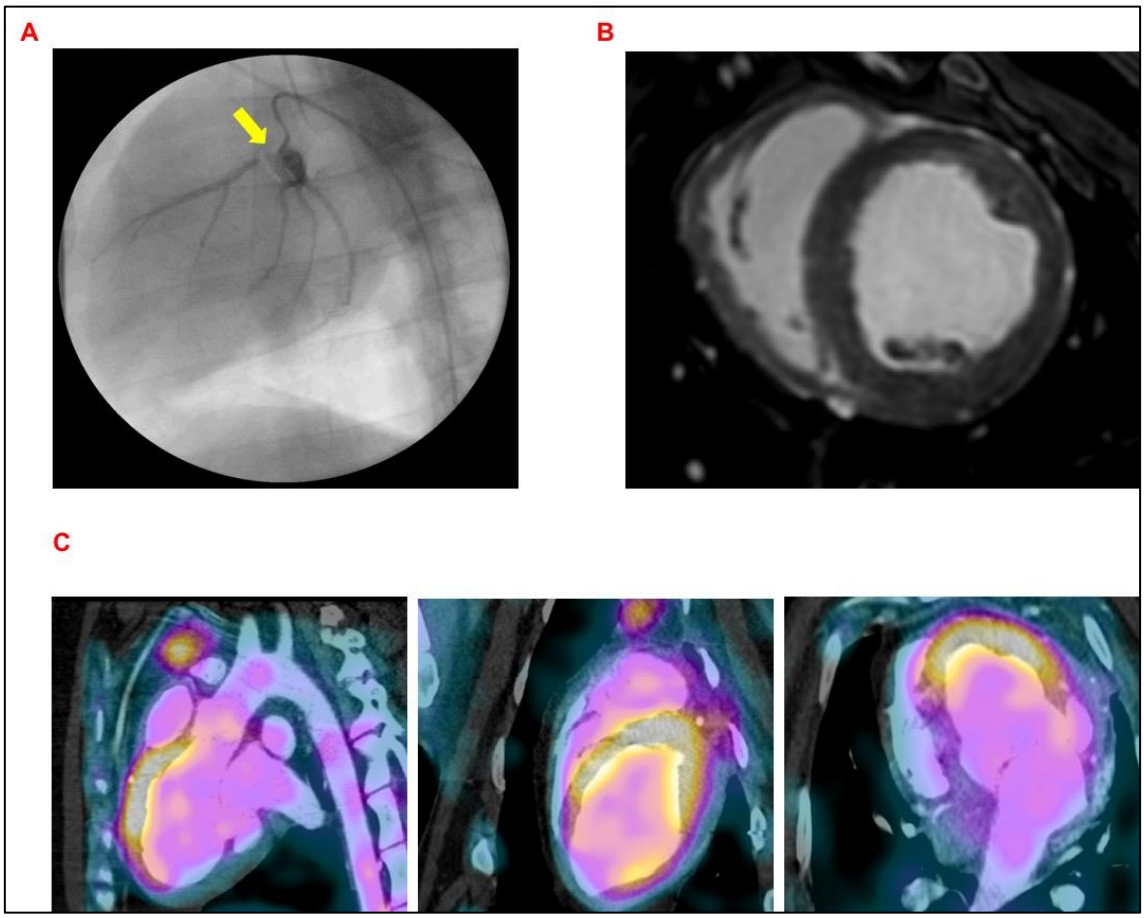

A: Coronary angiography showing severe LAD stenosis (yellow arrow points to the region of ameroid implant, generating severe stenosis). B Short axis slice of late gadolinium enhancement magnetic resonance imaging at medio-ventricular level. Subendocardial delayed enhanced region can be visualized occupying less than 50% of ventricular thickness. C: ^{18}F-FDG PET/CT at different projections showing cardiac glucose uptake in the anterior left ventricular wall.

<u>Figure 6.</u> Median and individual data of imaging-based parameters.

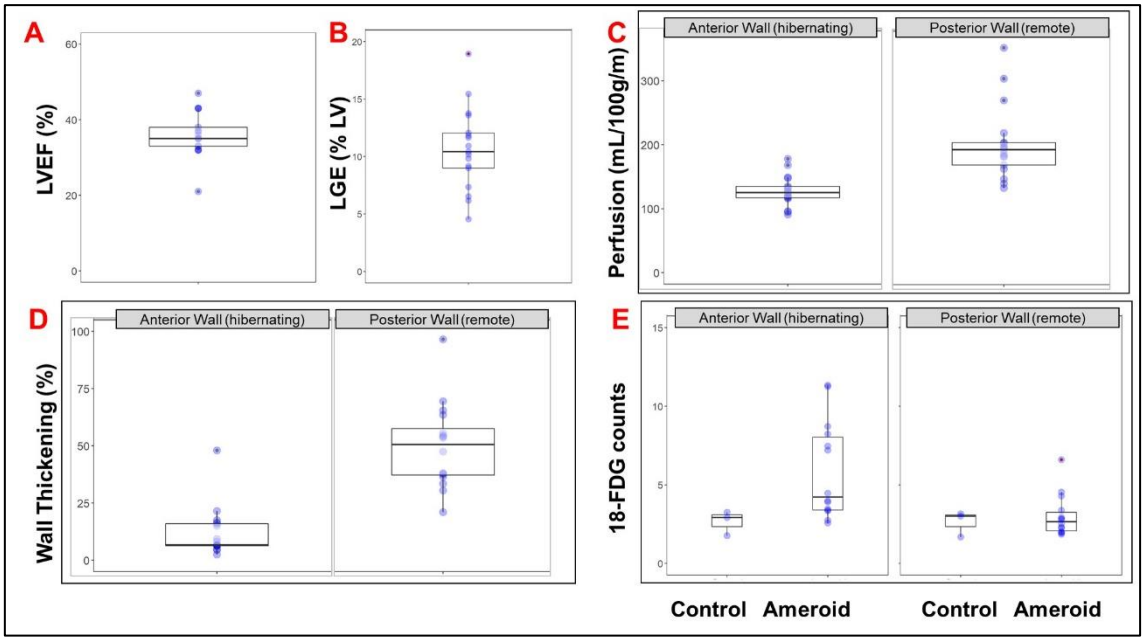

Left ventricular ejection fraction (panel A); late gadolinium enhancement magnetic resonance imaging (panel B), Wall thickening on CMR in the ischemic region (panel C) and in the non-ischemic region (panel D); Quantitative perfusion in the ischemic region (panel E) and in the non-ischemic region (panel F) Glucose uptake on ^{18}F-FDG counts (normalized to skeletal muscle counts) on PET/CT in the ischemic region (panel H), and in the remote non-ischemic region (panel G). Box-plot represents median, first and third quartile.

<u>Figure 7</u>. Contractile reserve of hibernating myocardium with dobutamine infusion

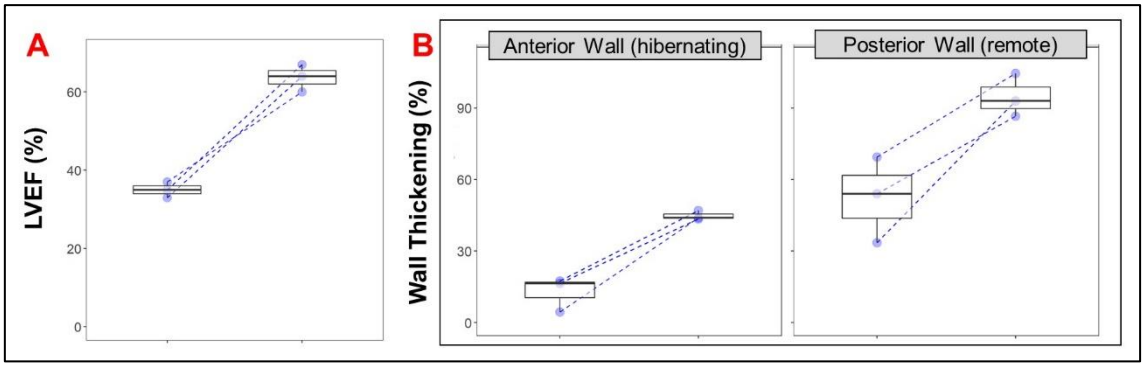

A: change in LVEF with dobutamine infusion. B: wall thickening change with dobutamine infusion at the antero-septal wall (hibernating myocardium)**.** C: wall thickening change with dobutamine infusion at the posterior wall (remote myocardium). Box-plot represents median, first and third quartile. Dots represent individual animals. Pre and post-dobutamine values from each animal are connected by dashed lines.

<u>Figure 8.</u> Histological evaluation of hibernating myocardium.

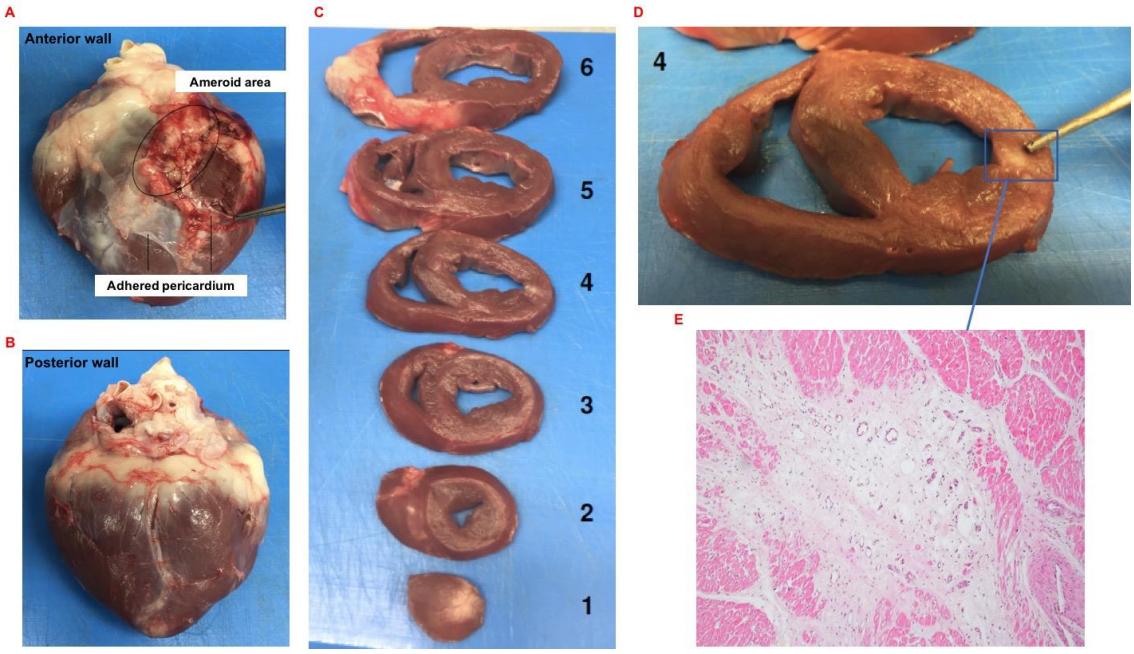

Ex-vivo images from an animal that completed the protocol. A: Macroscopic view of the LV anterior wall. B: Macroscopic view of LV posterior wall. C: Macroscopic view from 6 coronal slices from an operated heart. D: Coronal slice number 4 amplified showing minimal fibrosis (blue square) and viability of the LV anterior wall. E: Microscopic view of the fibrosis area from panel D.